

## CHAPTER IV

### HIGH SURFACE AREA TIN OXIDE VIA SOL-GEL PROCESS USING TIN GLYCOLATE PRECURSOR

#### 4.1 ABSTRACT

High surface area tin oxide was prepared via sol-gel process from the moisture stable tin glycolate precursor, synthesized directly from commercially available tin oxide and ethylene glycol via the oxide one-pot synthesis (OOPS) process using triethylenetetramine as base catalyst. The precursor was dissolved in 8 M HNO<sub>3</sub> at various HNO<sub>3</sub>/H<sub>2</sub>O ratios to form gels at room temperature. The effect of calcination time, calcination temperature, HNO<sub>3</sub>/H<sub>2</sub>O ratios and calcination heating rate were investigated. The structure of the obtained tin oxide was characterized using SEM, XRD and BET. The highest specific surface area tin oxide obtained was 510 m<sup>2</sup>/g at the HNO<sub>3</sub>:H<sub>2</sub>O ratio of 0.4, the calcination temperature and rate of 300°C and 0.5°C/min, respectively. Surface area of tin oxide products was decreased as increasing in the calcination temperature and the HNO<sub>3</sub>/H<sub>2</sub>O ratios while the crystallinity was undoubtedly increased.

KEYWORDS: Sol-gel process, Tin Oxide and Tin Glycolate

#### 4.2 INTRODUCTION

Intense interest has been focused on the investigation of metal alkoxides owing to their use as precursors in the sol-gel synthesis of inorganic metal oxides. High surface area tin oxide has been a subject of great interest due to its excellent properties, such as, high chemical and mechanical stabilities, high conductivity and low resistivity [1]. Among the various applications, many scientists have paid more attention on catalysts for methanol conversion and CO/O<sub>2</sub>, CO/NO reaction in the control of noxious emissions and gas sensors, which depend on crystallite size and specific surface area [1].

Sol-gel process is a method preferably used to prepare high surface area tin oxide because of the possibility to control its microstructure and homogeneity. More importantly, the process is easier to prepare three dimensional network metal oxides than other techniques at low temperature [4]. For example, Zhanget et al. [1] synthesized nanocrystalline tin oxide via the sol-gel process using granulated tin dissolving in  $\text{HNO}_3$  and added citric acid to slow down the hydrolysis and condensation. Specific surface area tin oxide of  $289 \text{ m}^2/\text{g}$  was obtained after calcinations at  $300^\circ\text{C}$  for 2 h. Wang et al. [5] synthesized mesostructured  $\text{SnO}_2$  using a cationic surfactant (cetyltrimethyl ammonium bromide, CTAB) as the organic supramolecular template and the hydrous tin chloride ( $\text{SnCl}_4 \cdot 5\text{H}_2\text{O}$ ) in  $\text{NH}_4\text{OH}$  as the inorganic precursor and counter ion, respectively, under acidic conditions at room temperature. The formation of tin oxide mesostructured material was proposed due to the presence of the hydrogen bonding interaction between supramolecular template and inorganic precursors  $\text{Sn}^{4+}$  and  $\text{OH}^-$ , which were supposed to self-assemble around the cationic surfactant molecules.

Recently, Wongkasemjit and coworkers have synthesized several metal alkoxides having moisture stable property, for example, titanium glycolate (Phonthammachai, 2003) [4] directly synthesized via the oxide one pot synthesis (OOPS) process from the reaction of commercially available titanium dioxide and ethylene glycol. The obtained alkoxide precursor containing ethylene glycolate ligands is hydrolytically stable, thus yielding more controllable sol-gel chemistry and minimizing special handling requirement.

In this work, tin alkoxide was thus emphasized and used as precursor for preparation of high surface area tin oxide. Tin glycolate was firstly synthesized from commercially available tin oxide and ethylene glycol using triethylene tetramine as base catalyst via the OOPS process. High surface area tin oxide was thus synthesized using tin glycolate as precursor via the sol-gel process. Various sol-gel processing conditions were investigated to obtain the optimal condition, as well.

## 4.3 EXPERIMENTAL

### 4.3.1 Materials

The starting material tin oxide ( $\text{SnO}_2$ , surface area of  $9.8 \text{ m}^2/\text{g}$ ) was purchased from Sigma-Aldrich Laborchemikalien GmbH. Ethylene glycol (EG) was obtained from Malinckrodt Baker, Inc. (USA). Triethylenetetramine (TETA) was purchased from Facai Polytech. Co. Ltd. (Bangkok, Thailand). Acetonitrile was supplied from Lab-Scan Company Co. Ltd. All chemicals were used as received.

### 4.3.2 Instrumental

Infrared absorption spectra (IR) were recorded on a Nicolet spectrometer with spectral resolution of  $4 \text{ cm}^{-1}$  using KBr mixed with sample. Characterization of crystal structure of products were obtained from a Rigaku X-ray diffractometer (XRD) system equipped with a RINT 2000 wide angle goniometer and a Cu tube for generating a  $\text{CuK}\alpha$  1 radiation ( $\lambda = 1.54 \text{ \AA}$ ) was used to obtain the X-ray diffraction patterns at a generator voltage of 40 kV and a generator current of 30 mA. Nickel filter was used as the  $\text{K}\beta$  filter. The goniometer parameters were divergence slit =  $1^\circ$  ( $2\theta$ ); scattering slit =  $1^\circ$  ( $2\theta$ ); and receiving slit = 0.3 nm. Sample was spread onto a glass slide. A scan speed of  $5^\circ$  ( $2\theta$ )/min with a scan step of  $0.02^\circ$  ( $2\theta$ ) was used during a continuous run in the  $5^\circ$  to  $70^\circ$  ( $2\theta$ ) range. The scanning electron micrographs were carried out to identify the microstructure of a sample. The samples were characterized using a JEOL 5200-2AE scanning electron microscope (SEM). Thermogravimetric analysis was carried out on a Perkin Elmer TG-DTA pyris diamond over  $30^\circ$ – $900^\circ\text{C}$  at a heating rate of  $10^\circ\text{C}/\text{min}$  under nitrogen atmosphere. The surface area of all samples was measured by the seven-point BET method using a Quantachrome Corporation Autosorp I. Before the measurement, a sample was outgassed by heating at 523 K for 4 h under vacuum to eliminate volatile adsorbents on the surface.

### 4.3.3 Synthesis of Tin Glycolate

Most importantly, tin glycolate is a newly synthesized and moisture stable precursor for the sol-gel process to obtain high surface area tin oxide. Tin glycolate was synthesized directly via the OOPS method from SnO<sub>2</sub>, EG and TETA used as base catalyst by following the method for titanium glycolate synthesis [4]. A mixture of SnO<sub>2</sub> (15.069 g, 0.01 mol) and TETA (14.62g, 0.01 mol) was stirred vigorously in excess EG (100 ml) and heated up to 200°C using silicone oil bath under nitrogen atmosphere for 24 h. The mixture solution was centrifuged to separate unreacted SnO<sub>2</sub> and the solution was vacuum distilled to remove excess EG and TETA to precipitate off crude product. The white solid product was washed with acetonitrile and dried in a vacuum desiccator for further characterizing using FT-IR, TGA, XRD and <sup>13</sup>C-NMR.

#### 4.3.4 Sol-gel Process of Tin Glycolate

Tin glycolate precursor (0.2217 g, 0.0928 mmol) was dissolved in various 8.0 M HNO<sub>3</sub>/H<sub>2</sub>O ratios. The ratio of HNO<sub>3</sub>/H<sub>2</sub>O was varied using the following formula; x μL of 8.0 M HNO<sub>3</sub>:y μL of H<sub>2</sub>O, where x:y = 1014:2535, 1014:2028 and 1014:1352 because gel can be formed without reversing to shrink gel at these three ratios at room temperature. The gel was dried at 110°C to obtain dried powder, followed by calcining at various temperatures (300°-900°C), times (2 to 6 h) and heating rate (0.1 to 1.0°C/min) to study the phase transformation. Tin oxide powder produced was characterized using SEM, TGA, BET and XRD.

## 4.4 RESULTS AND DISCUSSION

### 4.4.1 Synthesis of Tin Glycolate

The synthesized and purified tin glycolate precursor was identified using FT-IR, XRD, TGA and C<sup>13</sup>-NMR. FTIR spectrum of tin glycolate in figure 1 showed O-H stretching from ethylene glycol at the band around 3400-3300 cm<sup>-1</sup>, C-H stretching

of glycolate ligand at the band around  $2930\text{-}2830\text{ cm}^{-1}$ , C-O stretching around  $1077\text{ cm}^{-1}$ , Sn-O-C stretching at  $900\text{-}880\text{ cm}^{-1}$  and Sn-O stretching at the band around  $600\text{-}550\text{ cm}^{-1}$ . Thermal stability of tin glycolate precursor analyzed from TGA in figure 2 showed  $\sim 63.2\%$  ash yield at around  $300^\circ\text{-}400^\circ\text{C}$  corresponded to organic ligand decomposition under  $\text{N}_2$  which is closed to the theoretical value of  $63.1\%$  belonging to the structure of  $\text{Sn}(\text{OCH}_2\text{CH}_2\text{O})_2$ . Moreover, the solid state  $\text{C}^{13}$ -NMR spectrum, as shown in figure 3, clearly confirms the structure of tin glycolate at the chemical shift of  $62.5\text{ ppm}$  which is in a good agreement with a recent study on a solid-state NMR study of C-O-Sn moiety located at  $\sim 61.5\text{ ppm}$  [2]. XRD pattern of the synthesized tin glycolate precursor as compared to commercially starting material tin oxide in figure 4 indicated that the pattern is indeed belong to tin glycolate precursor.

#### 4.4.2 Characterization of Tin Oxide

The obtained tin oxide powder after gone through the sol-gel process was identified using XRD and SEM. The surface area was also measured using BET method. Since high surface area tin oxide preparation is the goal of most important this research, thus, effect of calcinations time/temperature,  $\text{HNO}_3/\text{H}_2\text{O}$  ratio and calcinations heating rate were carefully investigated.

##### 4.4.2.1 Effect of Calcinations Temperature

Firstly, investigation of calcinations temperature was varied from  $300^\circ$  to  $900^\circ\text{C}$  by fixing the other variables as follows:  $8\text{ M HNO}_3/\text{H}_2\text{O}$  ratio of  $0.4$ , heating rate of  $0.5^\circ\text{C}/\text{min}$  and calcinations time of  $4\text{ h}$ . XRD patterns in figure 5 showed that the crystallinity increased as increasing calcinations temperature. Nevertheless, surface areas of these products showed the same trend of the increase in crystallinity, giving decreasing value as increasing the calcinations temperature, as can be seen in table 1. XRD pattern of tin oxide after the sol-gel process and being calcined at  $300^\circ\text{C}$  showed tetragonal structure used for microsensor applications [1].

To ensure that other conditions would give the same trend, another conditions were experimented, as follows: 8 M HNO<sub>3</sub>/H<sub>2</sub>O ratio of 0.75, heating rate of 1.0°C/min and calcinations time of 2 h; 8 M HNO<sub>3</sub>/H<sub>2</sub>O ratio of 0.75, heating rate of 0.5°C/min and calcinations time of 2 h; 8 M HNO<sub>3</sub>/H<sub>2</sub>O ratio of 0.75, heating rate of 0.25°C/min and calcinations time of 2 h; and 8 M HNO<sub>3</sub>/H<sub>2</sub>O ratio of 0.5, heating rate of 1.0°C/min and calcinations time of 2 h. XRD results also showed the same trend as the first condition, as can be seen in figures 6-9 and table 2. As for the morphology of tin oxide products, as shown in figures 10-14, lower temperature showed amorphous phase along with crystalline phase and higher temperature showed more crystalline phase resulting in bigger crystallite size, less than 10 µm.

#### 4.4.2.2 Effect of Calcinations Time

The effect of calcinations time was observed for 2 conditions to find the suitable calcinations time giving pure tin oxide product. The first condition was 8 M HNO<sub>3</sub>/H<sub>2</sub>O ratio of 0.4, heating rate of 1.0°C/min and calcinations temperature of 300°C and the other was 8 M HNO<sub>3</sub>/H<sub>2</sub>O ratio of 0.75, heating rate of 1.0°C/min and calcinations temperature of 300°C. Calcinations time studied was ranged from 2, 3, 4 to 6h. It was found that for the first condition when increasing the calcinations time resulted in an increase in crystallinity, as can be seen in figure 15. Moreover, the calcinations time of 4 h gave more crystallinity than that of 6 h due to the agglomeration and destruction of crystals that showed crystallinity decreased and the surface area increased as showed in figure 15 and table 3, respectively. The second condition showed the increase in crystallinity as increasing calcinations time, see figure 16, and thus resulting in a decrease in the surface area (table 3). Calcinations time of 4h showed more crystalline phase than that of 6h. However, too longer time resulted in the phase transformation of tin oxide and became amorphous again. When comparing the surface area of tin oxide in various calcinations time, at 4h calcinations time the surface area of tin oxide at higher acid ratio, 0.75, is less than that of product at 0.4 acid ratio, meaning that acid concentration has affected to the surface area. Thus, the next effect studied was the 8 M HNO<sub>3</sub>/H<sub>2</sub>O ratio.

#### 4.4.2.3 Effect of Calcinations Heating Rate

The effect of calcinations heating rate on the tin oxide products was carried out using the condition of calcinations temperature and time of 300°C and 2 h, respectively, and HNO<sub>3</sub>/H<sub>2</sub>O ratio of 0.75. The calcinations heating rate was varied from 0.1°, 0.25°, 0.5° to 1.0°C/min. XRD results (Fig.21) showed increasing in crystallinity when the heating rate increased. However, too fast heating rate at 1.0°C/min indicated crystallite network due to too fast removal of organic residue, causing the structure of tin oxide to be collapsed. Specific surface area and morphology of crystallite at different heating rates in table 5 and in figure 22, respectively, showed not much different, but the 0.1°C/min calcinations rate gave high surface area. The reason was that lower heating rate provided a longer time for molecules to arrange themselves while removing organic residue from tin oxide three dimensional networks. However, too slow heating rate took too much time, thus it could be said that the appropriate heating rate was 0.5°C/min.

#### 4.4.2.4 Effect of 8 M HNO<sub>3</sub>/H<sub>2</sub>O ratio

The effect of acid concentration was determined in 2 conditions as follows; calcinations temperature, time and heating rate of 300°C, 4 h and 0.5°C/min, respectively, and of 300°C, 6 h 1.0°C/min, respectively, by varying the 8 M HNO<sub>3</sub>/H<sub>2</sub>O ratio from 0.4, 0.5 to 0.75 in both conditions. The results of both conditions were observed using BET, SEM and XRD. The XRD patterns (Fig.17-18) and SEM micrographs (Fig.19-20) obtained showed that when the HNO<sub>3</sub>/H<sub>2</sub>O ratio increased the crystallinity became sharper. This is due to the acid acting as a catalyst and hydrolyzing the alkoxide ligands [4]. When the acid concentration increases, the hydrolysis and condensation rates of some molecules occur faster, shortening gelation time, as a result, giving a shorter branched tin oxide network, as can be confirmed by the decrease of surface area (Table 4) in the following order; 0.4>0.5>0.75. Thus, for the highest surface area, 510 m<sup>2</sup>/g, it can be concluded that the suitable acid ratio was at the 0.4 HNO<sub>3</sub>/H<sub>2</sub>O ratio.

#### 4.5 CONCLUSIONS

In this thesis work, high surface area tin oxide was successfully synthesized using tin glycolate as the precursor via the sol-gel process. The gel can be formed at room temperature using 8M HNO<sub>3</sub>. The HNO<sub>3</sub>/H<sub>2</sub>O ratio, calcinations time and calcinations temperature have affected to the crystal structure of the resulted tin oxide. The calcinations temperature and HNO<sub>3</sub>/H<sub>2</sub>O ratio had a substantial influence on the crystallinity and surface area. Increase of temperature and HNO<sub>3</sub>/H<sub>2</sub>O ratio result higher crystallinity, but lower specific surface area. The highest surface area of ~ 510 m<sup>2</sup>/g can be obtained when using suitable condition as follows; the lowest calcinations temperature, time and heating rate of 300°C, 4 h and 0.5°C/min, respectively, and 0.4 HNO<sub>3</sub>/H<sub>2</sub>O ratio.

#### 4.6 ACKNOWLEDGEMENTS

This research work is supported by the Postgraduate Education and Research Program in Petroleum and Petrochemical Technology (ADB Fund, ADB consortium) Ratchadapisake Sompote Fund, Chulalongkorn University and The Thailand Research Fund (TRF).

#### 4.7 REFERENCES

- [1] Esfandyarpour B., Asl oleimani E. Nanocrystalline Thin Film Tin-Oxide ensors Compatible With Post CMO Processing.
- [2] Jiang X., Wang Y., Herricks T., Xia Y. (2004). Ethylene glycol-mediated synthesis of metal oxide nanowires. Journal of Material Chemistry, 14, 695-703
- [3] Ksapabutr B., Gulari E., Wongkasemjit S. (2004). One-pot synthesis and characterization of novel sodium tris(glycozirconate) and cerium glycolate precursors and their paralysis. Materials Chemistry and Physics, 83, 34-42.
- [4] Phonthammachai, N., Chairassameewong, T., Gulari, E., Jamieson, A.M., and Wongkasemjit, S. (2003). Structural and rheological aspect of mesoporous



nanocrystalline TiO<sub>2</sub> synthesized via sol-gel process. Microporous and Mesoporous Materials, 66, 261-271.

- [5] Wang, Y.D., Ma, C.L., Wu, X.H., Sun, X.D., Li, H.D. (2002). Electrical and gas sensing properties of mesostructured tin oxide-based H<sub>2</sub> sensor. Sensors and Actuators, B85, 270-276.
- [6] Zhang, J., Gao, L. (2004). Synthesis and characterization of nanocrystalline tin oxide by sol-gel method. Journal of Solid State Chemistry, 177, 1425-1430.

**Table 1** Specific surface area of the tin oxide synthesized by the sol-gel method various calcinations temperatures by fixing (a) 0.5°C/min, 4h calcinations rate and time, respectively, and 0.4 HNO<sub>3</sub>/H<sub>2</sub>O ratio, (b) 1.0°C/min, 2h calcinations rate and time, respectively, and 0.75 HNO<sub>3</sub>/H<sub>2</sub>O ratio, (c) 0.5°C/min, 2h calcinations rate and time, respectively, and 0.75 HNO<sub>3</sub>/H<sub>2</sub>O ratio, (d) 0.25°C/min, 2h calcinations rate and time, respectively, and 0.75 HNO<sub>3</sub>/H<sub>2</sub>O ratio and (e) 1.0°C/min, 2h calcinations rate and time, respectively, and 0.5 HNO<sub>3</sub>/H<sub>2</sub>O ratio

Temperature (°C)	Specific Surface Area ( m <sup>2</sup> /g)				
	(a)	(b)	(c)	(d)	(e)
300	265.17	168.45	152.9	168.8	234.1
400	96.35	139.3	74.56	112.4	139.3
500	80.14	170.1	52.14	61.25	168.6
600	59.53	105.9	-	-	-
700	50.52	25.75	-	-	-
900	27.2	27.52	-	-	-

**Table 2** Specific surface area of the tin oxide synthesized by the sol-gel method at various calcinations time by fixing calcinations temperature and rate at 300°C and 1.0°C/min, respectively, using the HNO<sub>3</sub>/H<sub>2</sub>O ratio of (a) 0.4 and (b) 0.75

Time (h)	Specific Surface Area ( m <sup>2</sup> /g)	
	(a)	(b)
2	234.1	152.19
3	238.3	225.0
4	173.9	155.2
6	203.7	246.8

**Table 3** Specific surface area of the tin oxide synthesized by sol-gel method at various calcination heating rate by fix 300°C , 2 h and 0.75 of HNO<sub>3</sub>/H<sub>2</sub>O ratio

Calcination heating rate ( °C/min)	Specific Surface Area ( m <sup>2</sup> /g)
0.1	200.3
0.25	168.8
0.5	152.19
1.0	168.45

**Table 4** Specific surface area of the tin oxide synthesized by the sol-gel method at various HNO<sub>3</sub>/H<sub>2</sub>O ratios and calcinations temperature, rate and time of (a) 300°C, 1.0°C/min, 6h and (b) 300°C, 0.5°C/min, 4 h

7.5 M HNO <sub>3</sub> /H <sub>2</sub> O ratio	Specific Surface Area ( m <sup>2</sup> /g)	
	(a)	(b)
0.4	203.7	510.3
0.5	196.5	218.1
0.75	215.3	155.2

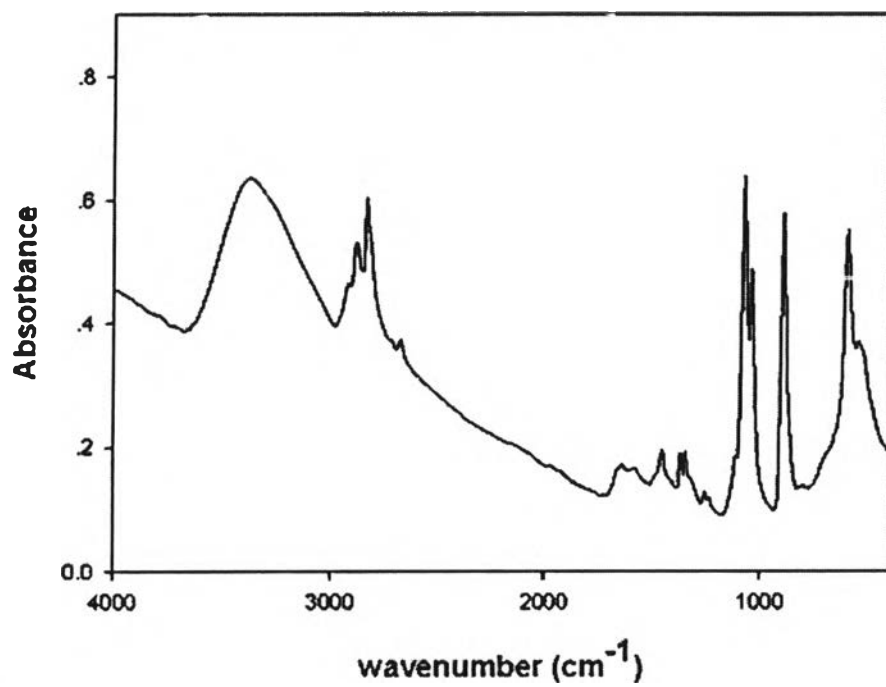


**Figure 1** IR spectrum of tin glycolate.

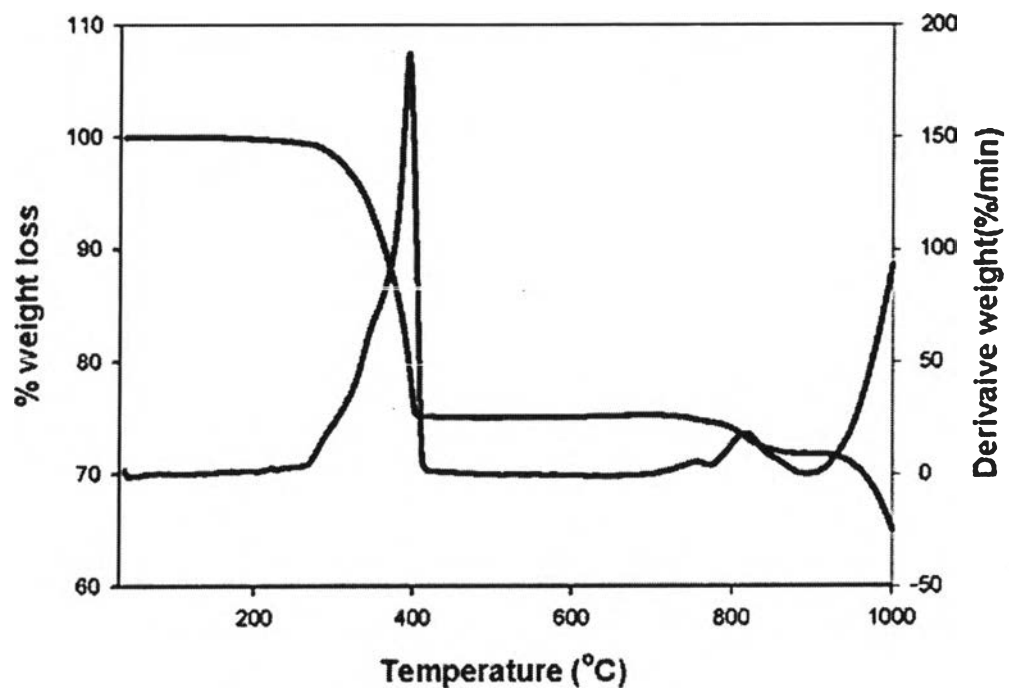
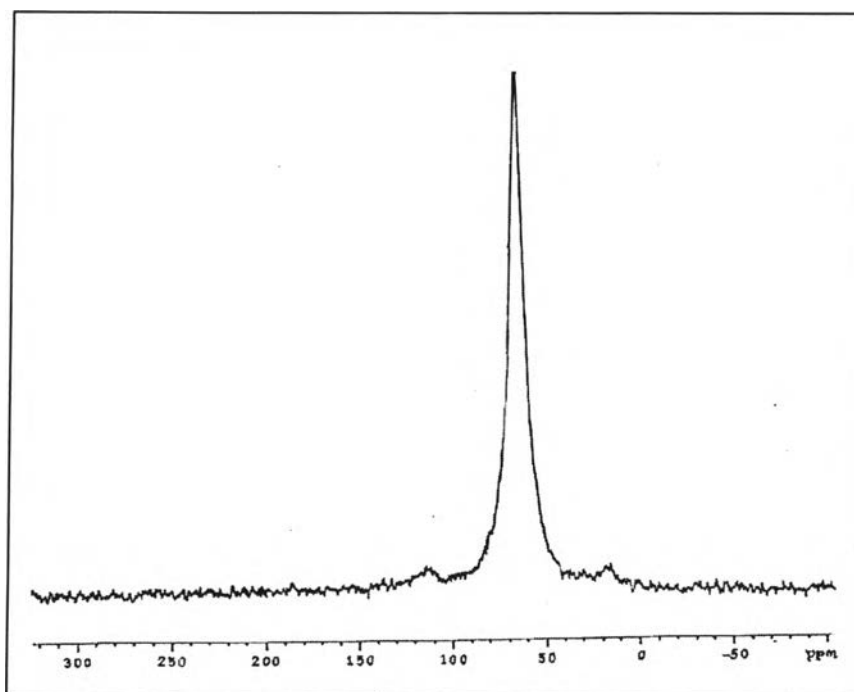
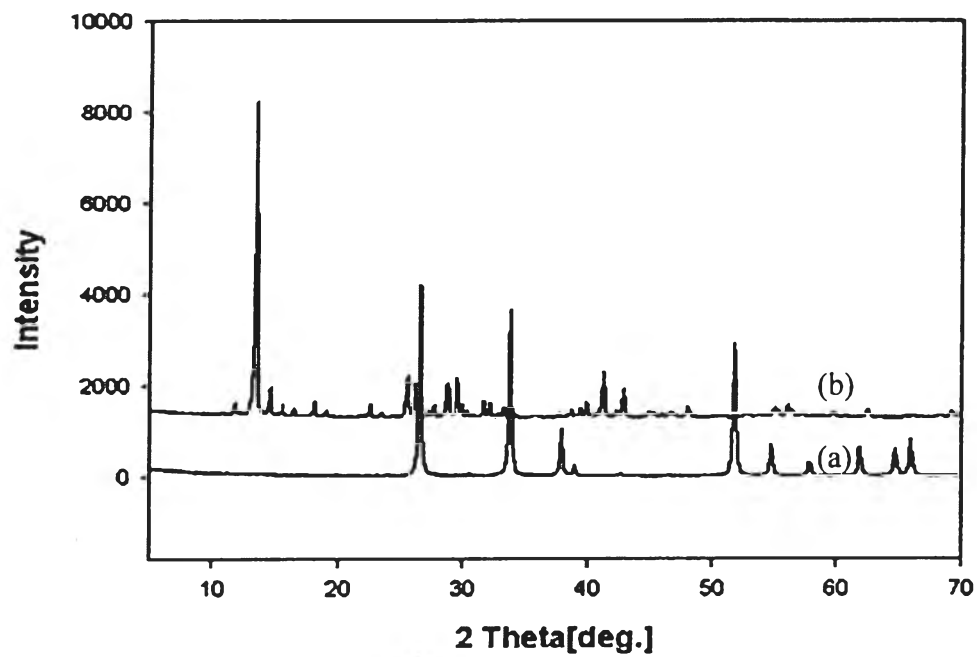


Figure 2 TGA profile of tin glycolate.



**Figure 3**  $\text{C}^{13}$ -NMR spectrum of tin glycolate.





**Figure 4** XRD patterns of (a) commercial  $\text{SnO}_2$  and (b) synthesized  $\text{Sn}(\text{OCH}_2\text{CH}_2\text{O})_2$  precursor.

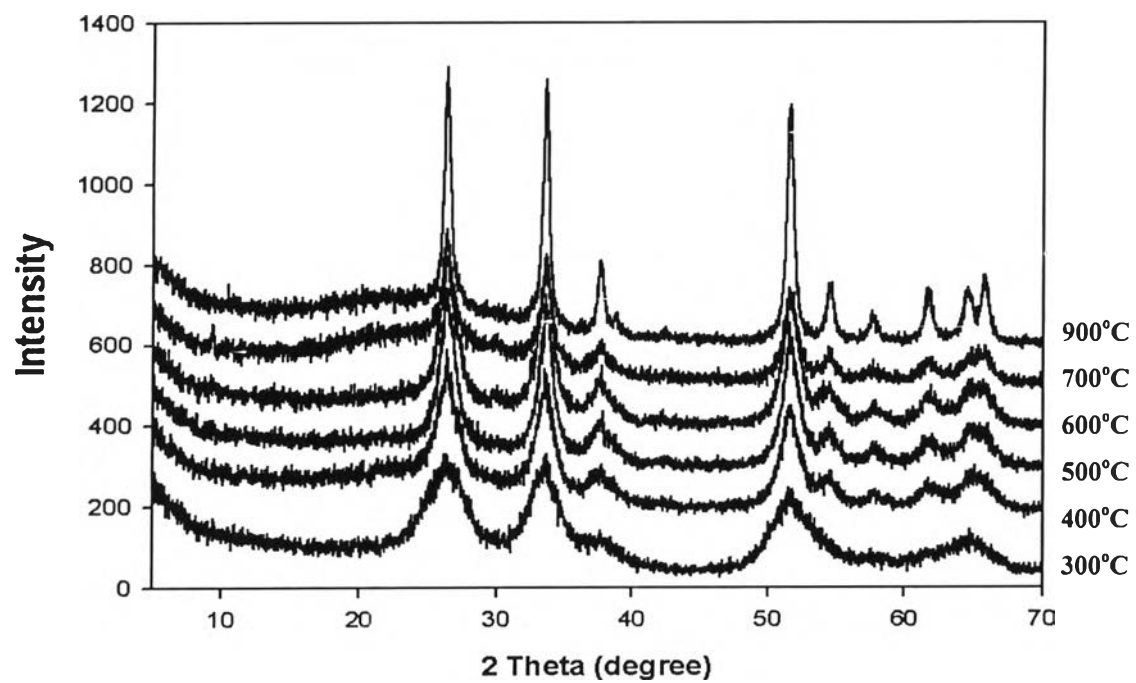


**Figure 5** XRD patterns of tin oxide calcined at different temperatures from 300° to 900°C for 4h by fixing 0.5°C/min calcinations rate and 0.4 HNO<sub>3</sub>/H<sub>2</sub>O ratio.

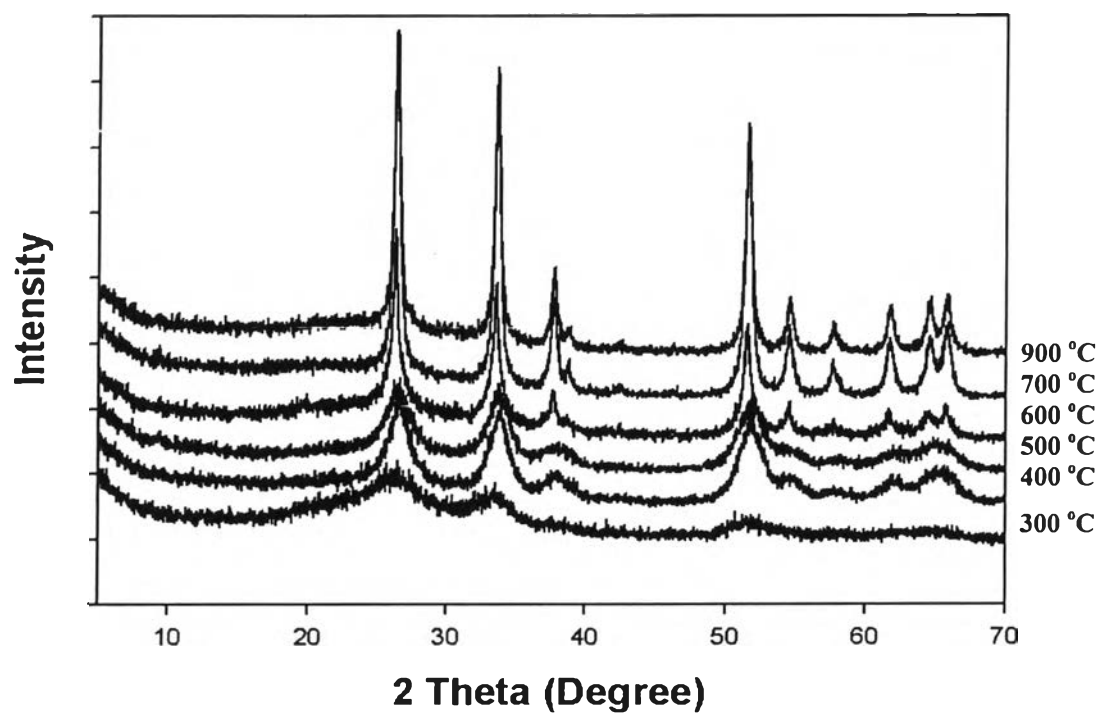


**Figure 6** XRD patterns of tin oxide calcined at different temperatures from 300° to 900°C for 2h by fixing 1.0°C/min calcinations rate and 0.75 HNO<sub>3</sub>/H<sub>2</sub>O ratio.

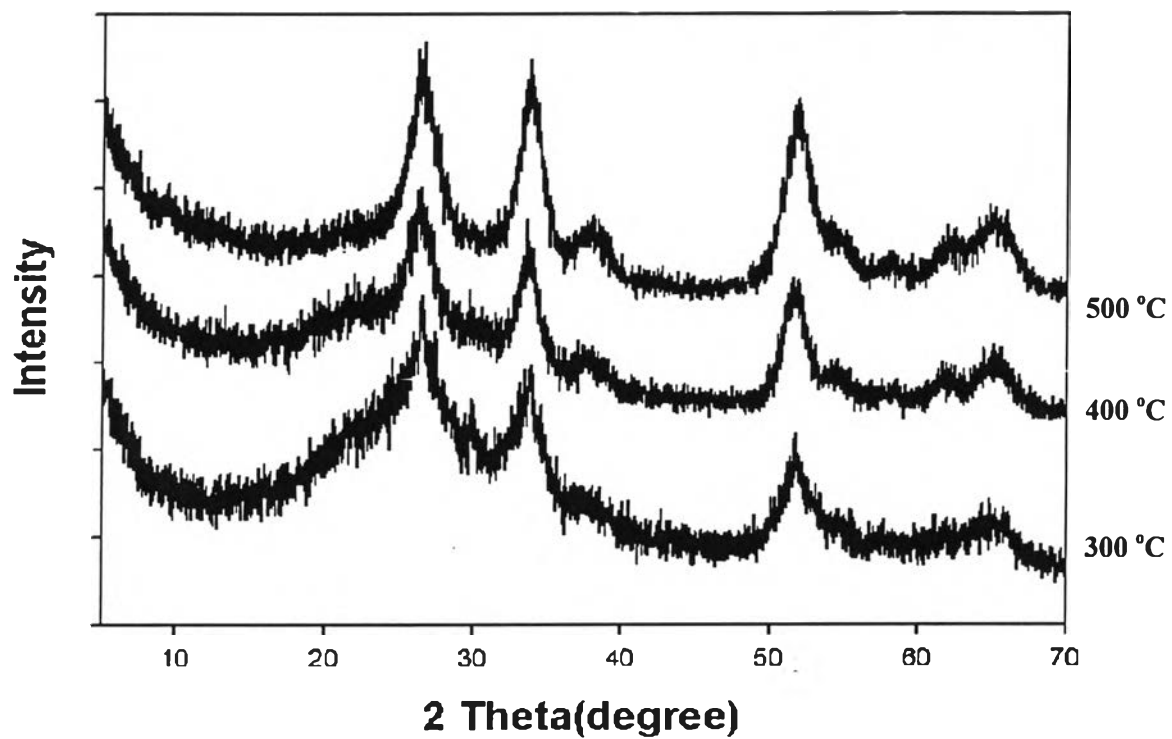


**Figure 7** XRD patterns of tin oxide calcined at different temperatures from 300° to 500°C for 2h by fixing 0.5°C/min calcinations rate and 0.75 HNO<sub>3</sub>/H<sub>2</sub>O ratio.

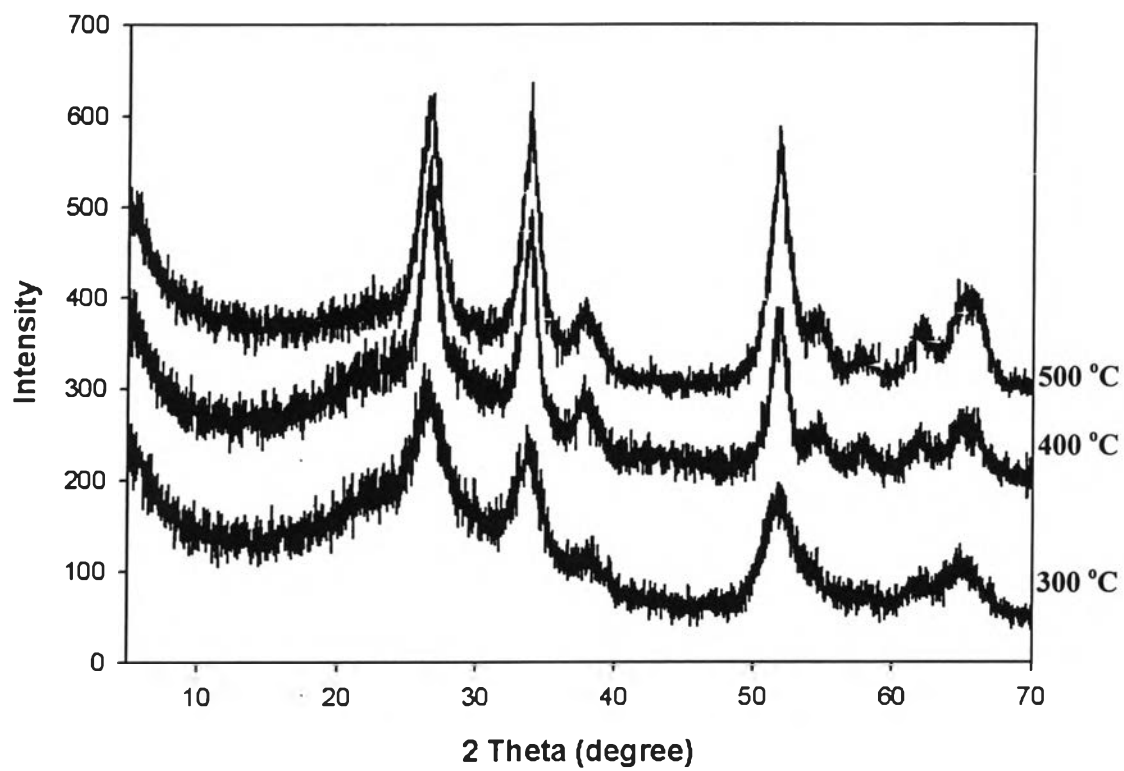


**Figure 8** XRD patterns of tin oxide calcined at different temperatures from 300° to 500°C for 2h by fixing 0.25°C/min calcinations rate and 0.75 HNO<sub>3</sub>/H<sub>2</sub>O ratio.

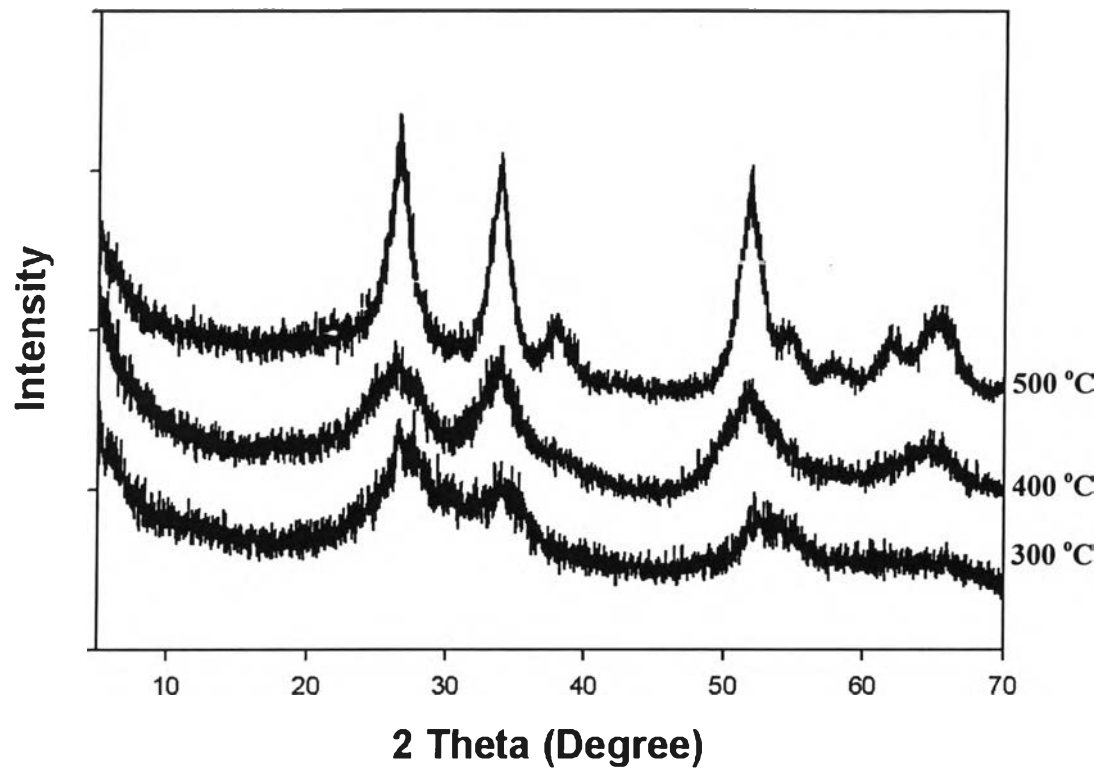


**Figure 9** XRD patterns of tin oxide calcined at different temperatures from 300° to 500°C for 2h by fixing 1.0°C/min calcinations rate and 0.5 HNO<sub>3</sub>/H<sub>2</sub>O ratio.

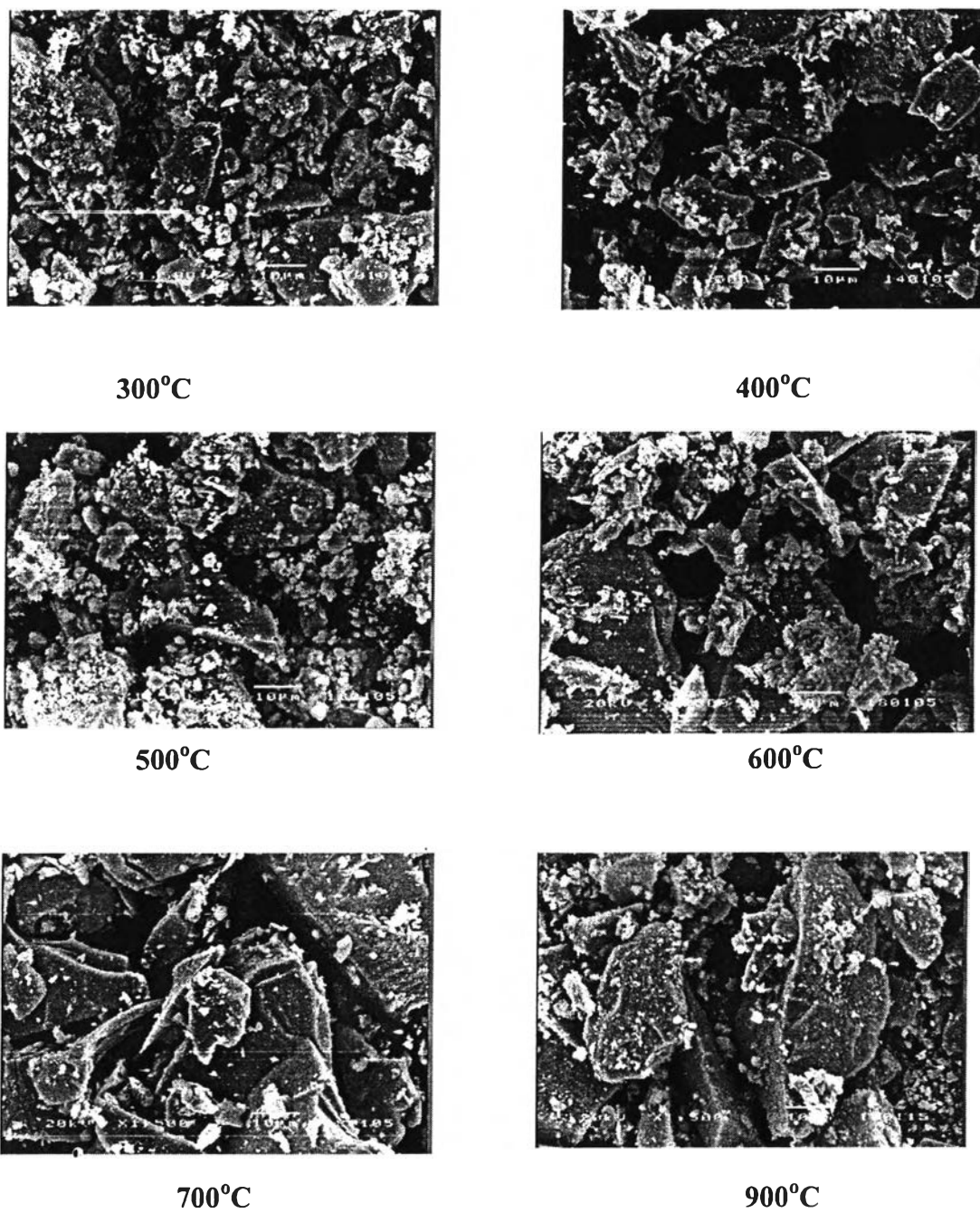


**Figure 10** SEM images of calcined SnO<sub>2</sub> at different calcinations temperatures from 300° to 900°C for 4h by fixing 0.5°C/min calcinations rate and 0.4 HNO<sub>3</sub>/H<sub>2</sub>O ratio.

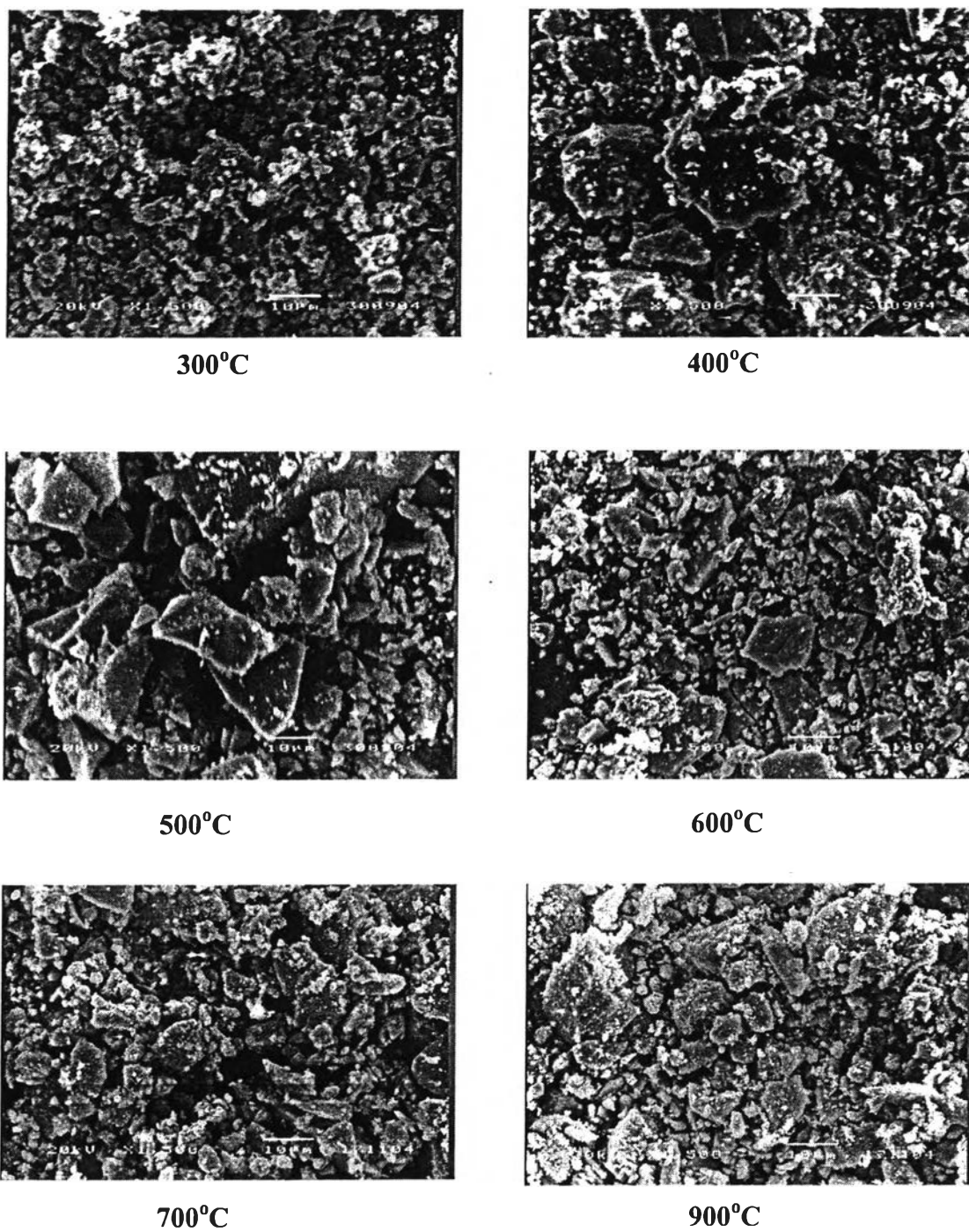


**Figure 11** SEM images of calcined SnO<sub>2</sub> at different calcinations temperature from 300° to 900°C for 2h by fixing 1.0°C/min calcinations rate and 0.75 HNO<sub>3</sub>/H<sub>2</sub>O ratio.



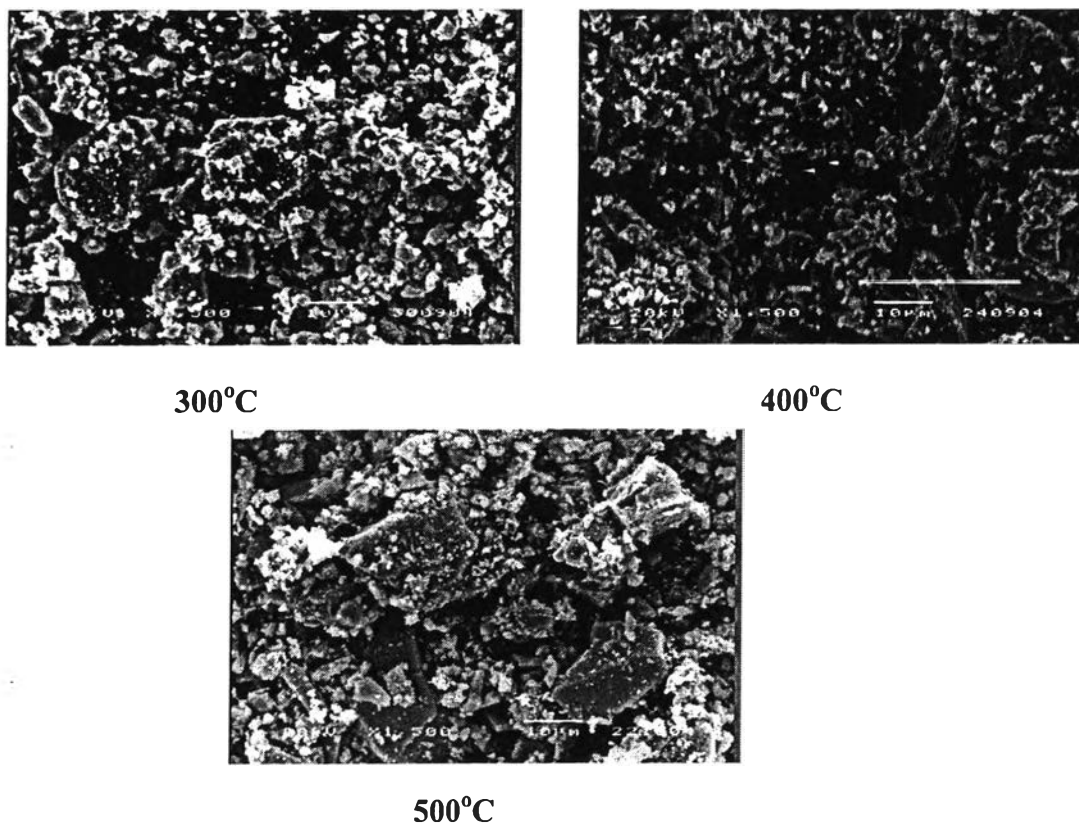


**Figure 12** SEM images of calcined  $\text{SnO}_2$  at different calcinations temperatures from  $300^\circ$  to  $500^\circ\text{C}$  for 2h by fixing  $0.5^\circ\text{C}/\text{min}$  calcinations rate and 0.75  $\text{HNO}_3/\text{H}_2\text{O}$  ratio.

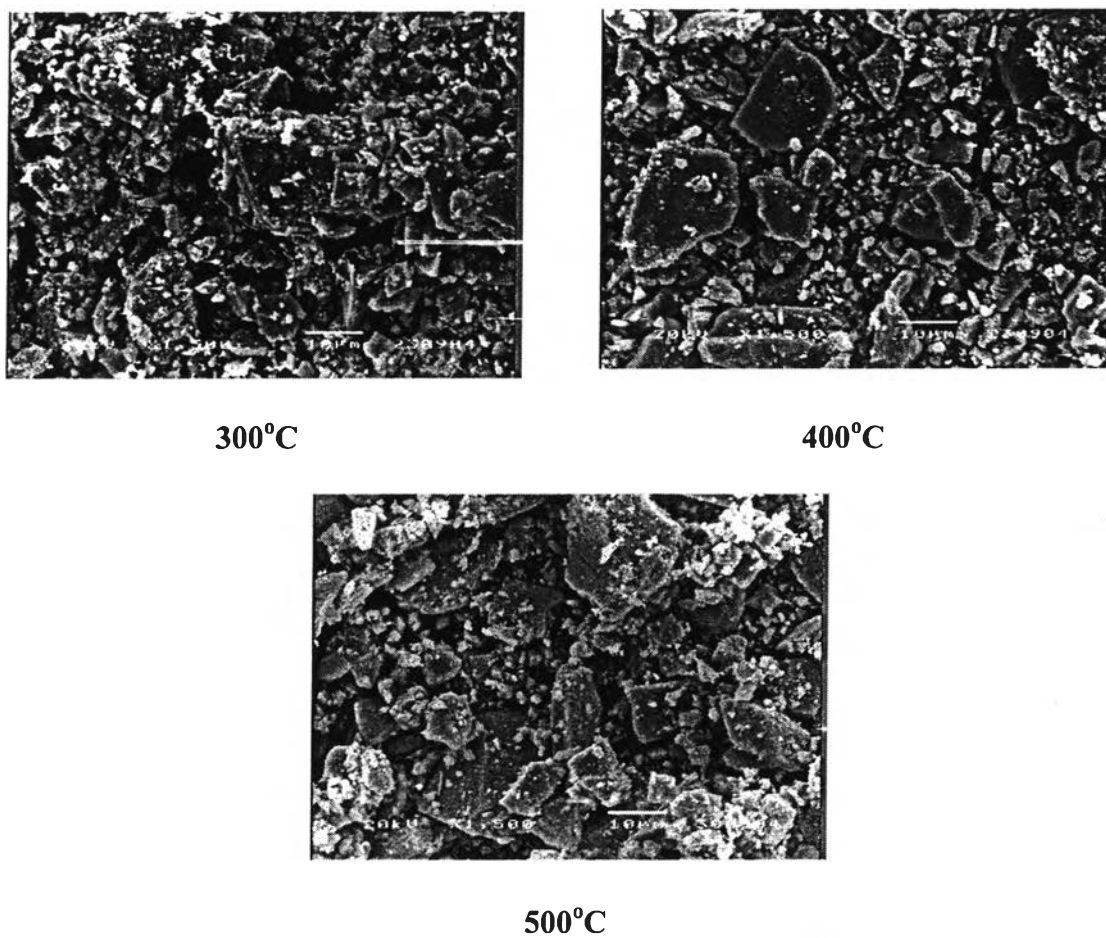


**Figure 13** SEM images of calcined  $\text{SnO}_2$  at different calcinations temperatures from  $300^\circ$  to  $500^\circ\text{C}$  for 2h by fixing  $0.25^\circ\text{C}/\text{min}$  calcinations rate and 0.75  $\text{HNO}_3/\text{H}_2$  ratio.

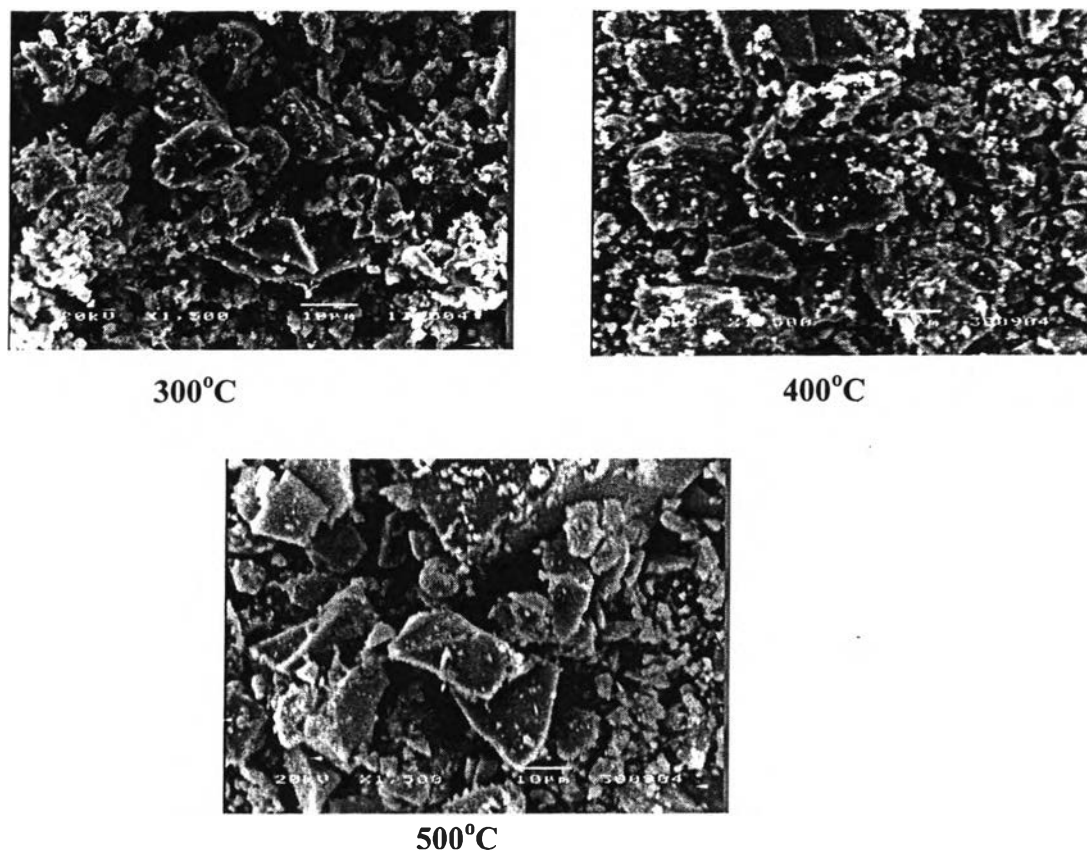


**Figure 14** SEM images of calcined  $\text{SnO}_2$  at different calcinations temperatures from  $300^\circ$  to  $500^\circ\text{C}$  for 2h by fixing  $1.0^\circ\text{C}/\text{min}$  calcinations rate and 0.5  $\text{HNO}_3/\text{H}_2\text{O}$  ratio.

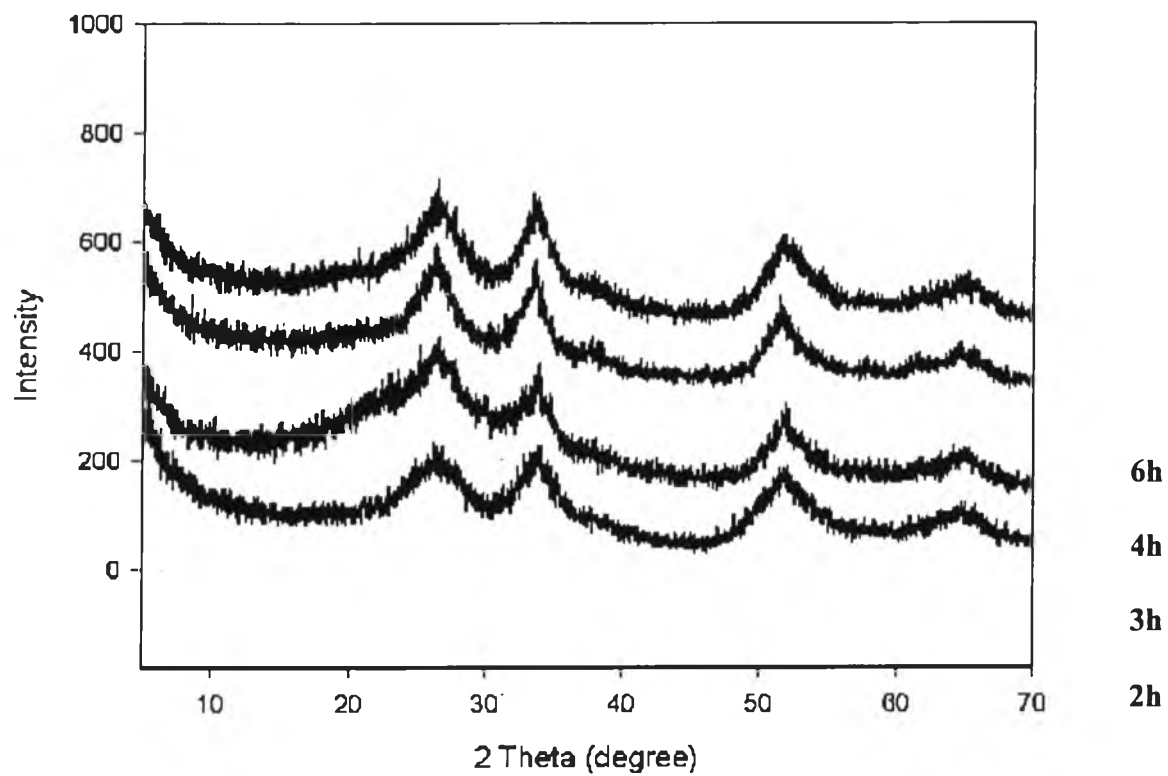


**Figure 15** XRD patterns of tin oxide calcined at different calcination times from 2 to 6h at 300°C and 1.0°C/min calcinations temperature and rate, respectively, and 0.4 HNO<sub>3</sub>/H<sub>2</sub>O ratio.

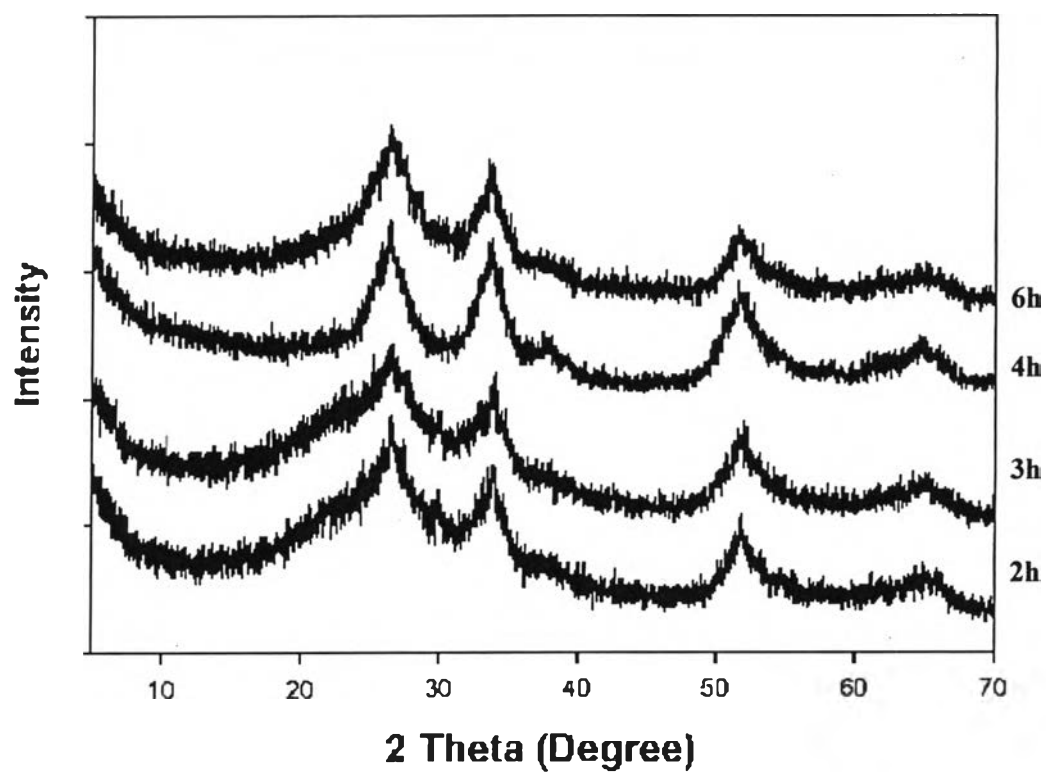


**Figure 16** XRD patterns of tin oxide calcined at different calcination time from 2 to 6h at  $300^\circ\text{C}$  and  $1.0^\circ\text{C}/\text{min}$  calcinations temperature and rate, respectively, and 0.75  $\text{HNO}_3/\text{H}_2\text{O}$  ratio.

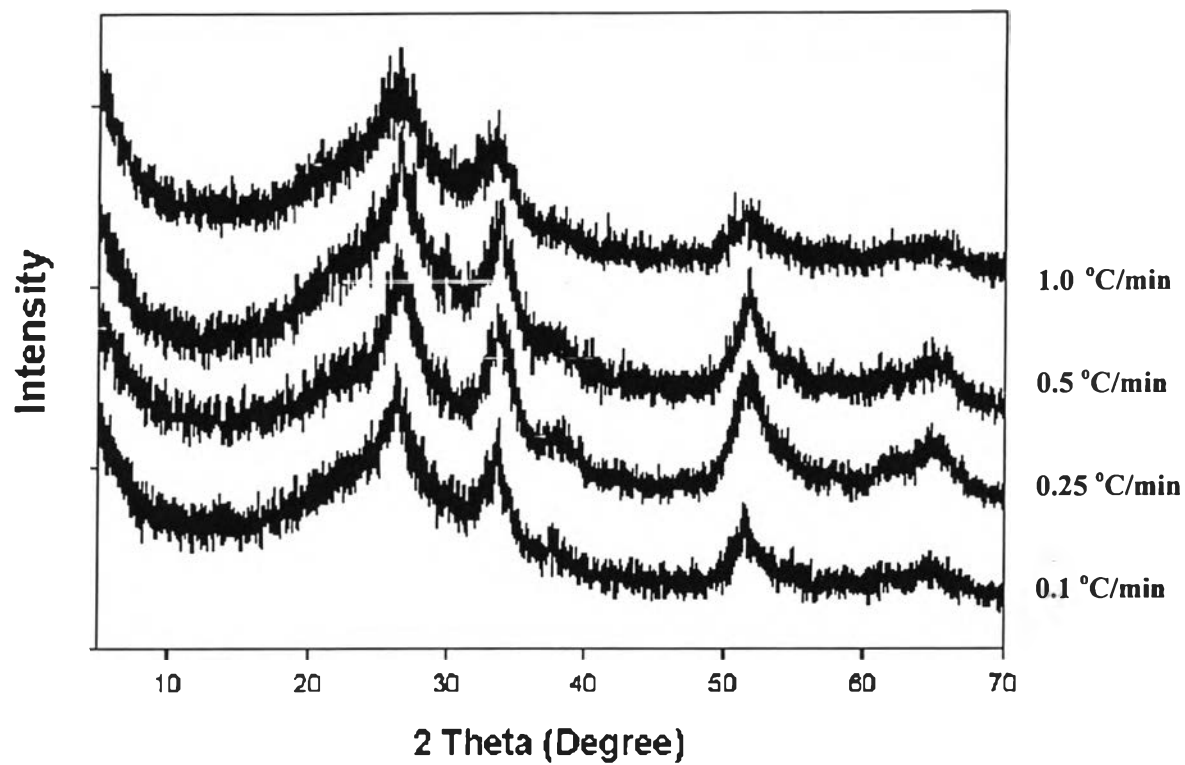


**Figure 17** XRD patterns of tin oxide calcined at calcination heating rate from 0.1° to 1.0°C/min at 300°C and 4h calcinations temperature and time, respectively, and 0.75 HNO<sub>3</sub>/H<sub>2</sub>O ratio.

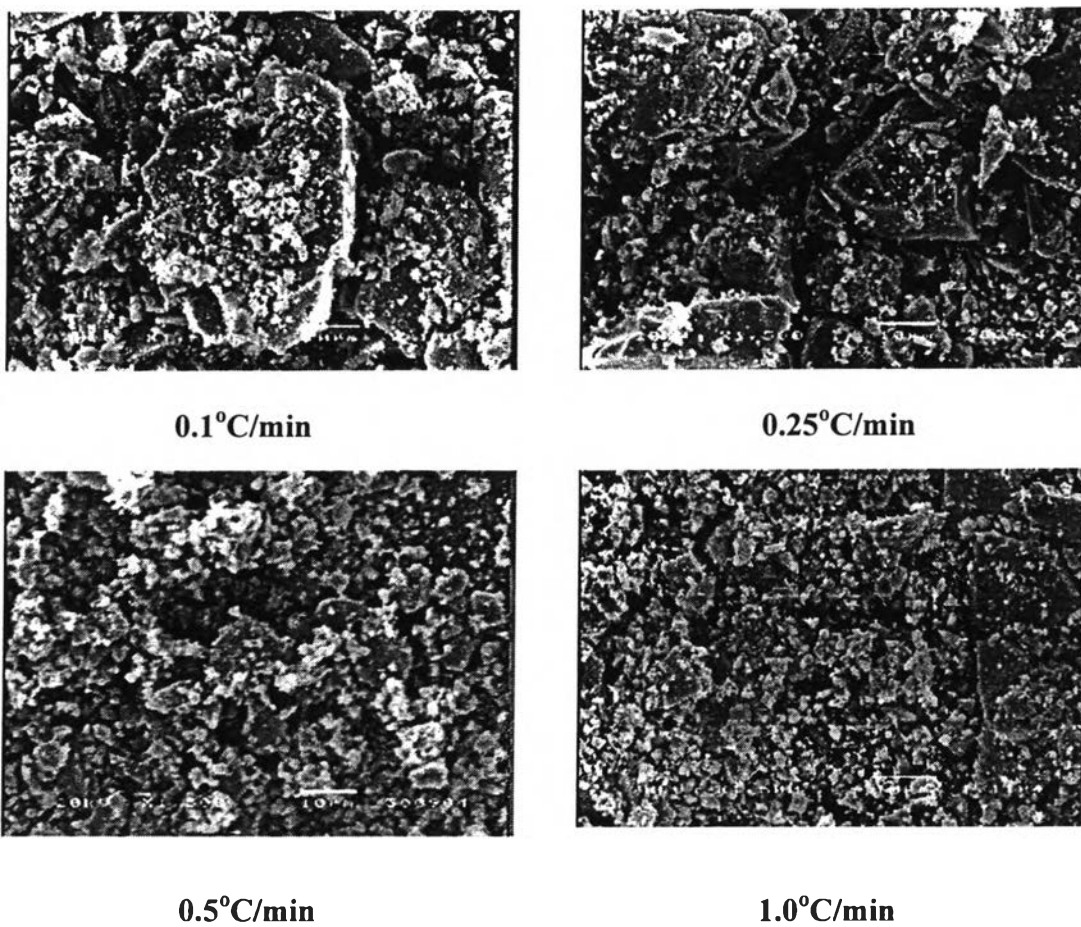


**Figure 18** SEM images of calcined SnO<sub>2</sub> at calcination heating rate from 0.1° to 1.0°C/min at 300°C and 4h calcinations temperature and time, respectively, and 0.75 HNO<sub>3</sub>/H<sub>2</sub>O ratio.

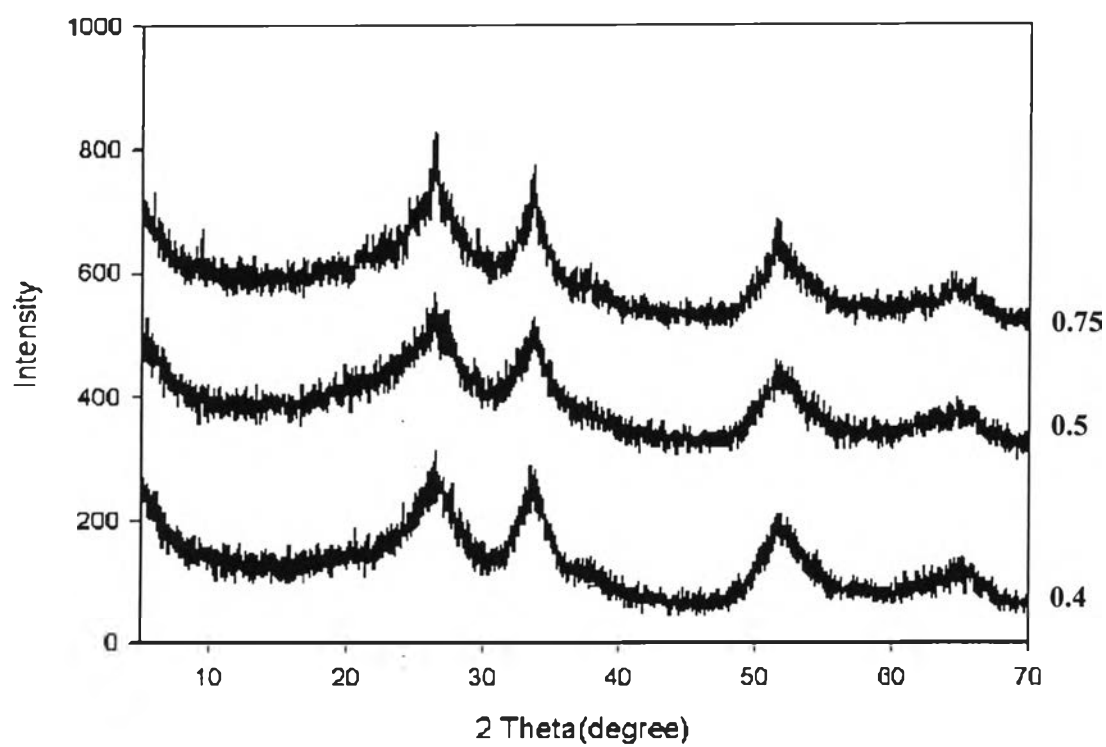


**Figure 19** XRD patterns of tin oxide calcined at different of  $\text{HNO}_3/\text{H}_2\text{O}$  ratios from 0.4 to 0.75 at  $300^\circ\text{C}$ , 4h and  $0.5^\circ\text{C}/\text{min}$  calcinations temperature, time and rate, respectively.



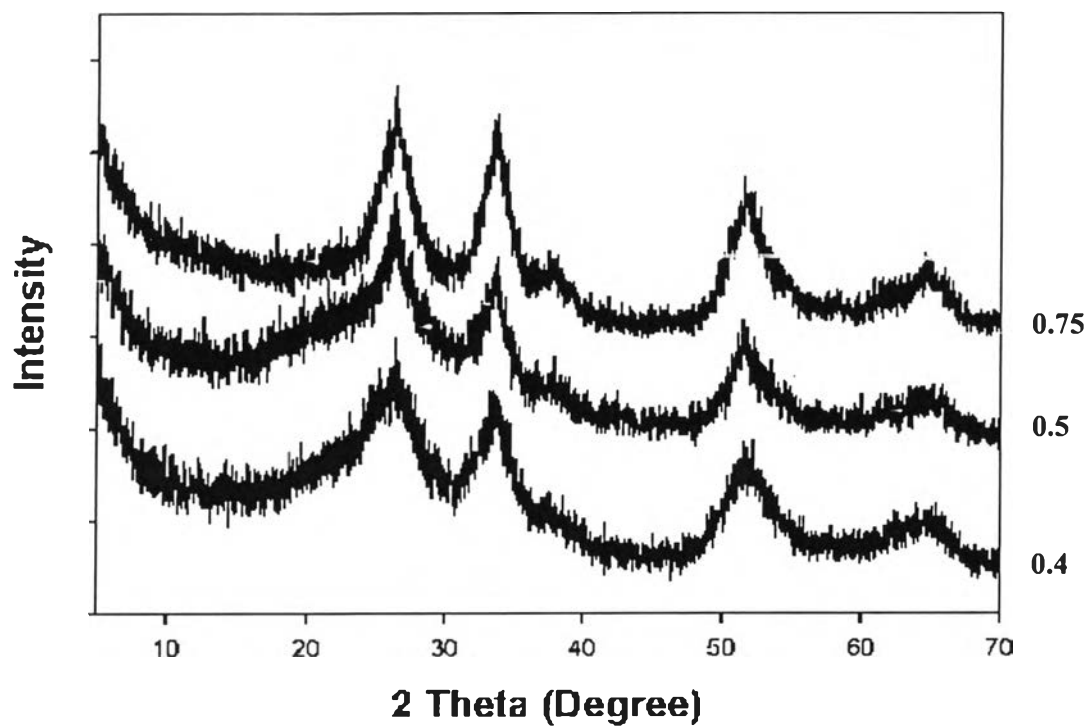
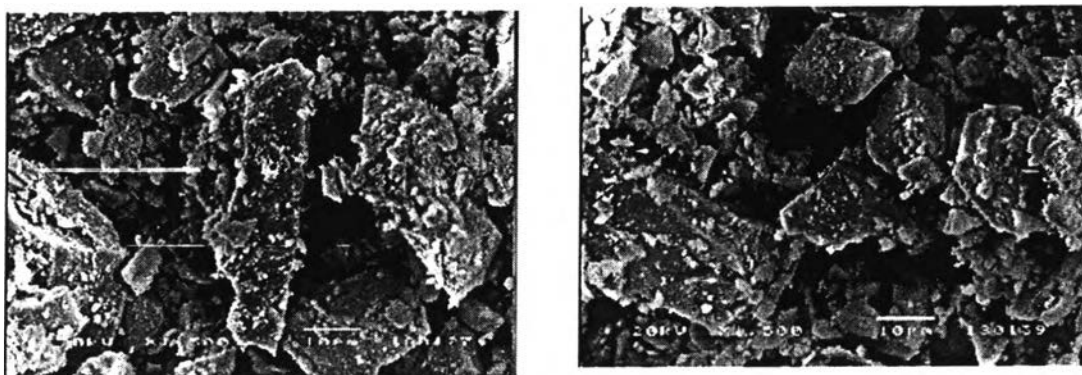
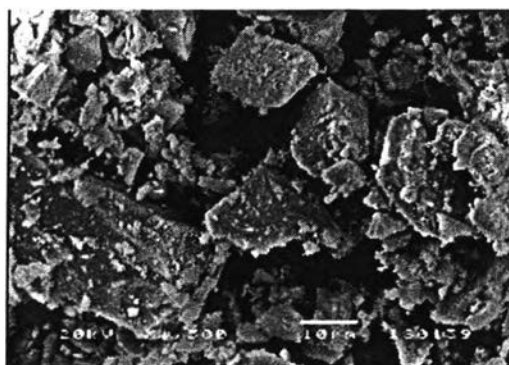


**Figure 20** XRD patterns of tin oxide calcined at different of HNO<sub>3</sub>/H<sub>2</sub>O ratios from 0.4 to 0.75 at 300°C, 6h and 1.0°C/min calcinations temperature, time and rate, respectively.



0.4

0.5



0.75

**Figure 21** SEM images of calcined SnO<sub>2</sub> at different HNO<sub>3</sub>/H<sub>2</sub>O ratios from 0.4 to 0.75 at 300°C, 4h and 0.5°C/min calcinations temperature, time and rate, respectively.

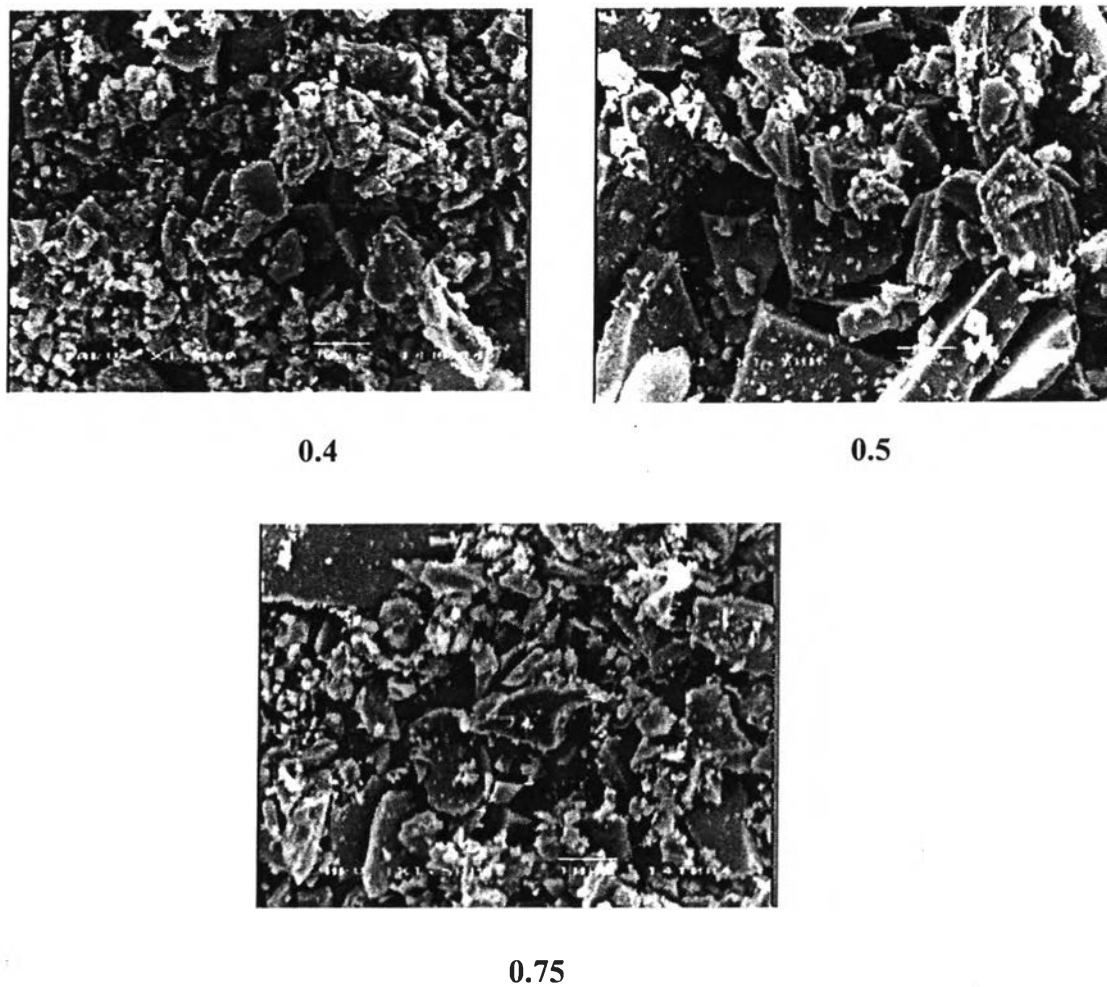


**Figure 22** SEM images of calcined  $\text{SnO}_2$  at different  $\text{HNO}_3/\text{H}_2\text{O}$  ratios from 0.4 to 0.75 at  $300^\circ\text{C}$ , 6h and  $1.0^\circ\text{C}/\text{min}$  calcinations temperature, time and rate, respectively.